

# A comparison on initial-value ray tracing and fast marching eikonal solver for VTI traveltimes computing

S.Y. Moussavi Alashloo<sup>1,\*</sup>, D.P. Ghosh<sup>1</sup>, Y. Bashir<sup>1</sup> and W.I. Wan Yusoff<sup>1</sup>

<sup>1</sup> Department of Petroleum Geoscience, Universiti Teknologi PETRONAS, Sri Iskandar, Malaysia

E-mail: y.alashloo@gmail.com

**Abstract.** The Earth's subsurface is an anisotropic medium where the velocity of seismic waves alters in different propagation angles. Omitting anisotropy in seismic imaging not only brings mis-positioning of migrated dipping events but also fails to retain dipping energy during dip-moveout. To account for the efficacy of seismic anisotropy in imaging, an anisotropic wave equation must be engaged. Seismic traveltimes computing is fundamental of both Kirchhoff migration and tomography algorithms. Two main categories of traveltimes computing involve traditional ray tracing methods and finite difference eikonal solvers. In this study, we present two techniques of initial-value ray tracing and fast marching eikonal solver in isotropic and vertical transverse isotropy (VTI) media, and a comparison between results is demonstrated for more evaluation. Although the ray tracing approach is able to compute multiple arrivals with great precision, the eikonal solver is faster and more robust for traveltimes computation. Since the ray tracing result is not a deterministic solution and it depends on the initial circumstance, employing the eikonal solver method are more preferred and suggested.

## 1. Introduction

Hydrocarbon and geothermal reservoirs, and overlying strata are comprised anisotropic rocks. Considering anisotropy into account is necessary not only to avoid distortions in imaging, but also provides important information about lithology and fracture networks. One of the causes of anisotropy in sedimentary rocks is the thin layering. If the structure has horizontal layers, it is a TI medium with vertical axis of symmetry (VTI). One of the challenging problems in seismic imaging is the calculation of time taken by seismic wave for traveling from source to receiver. In P-wave velocity analysis and imaging, several traveltimes computing algorithms have been developed for VTI condition [1-3]. There are two principal classes of traveltimes computing which include ray tracing and eikonal solver methods.

The ray technique was firstly employed to study the propagation of the high-frequency elastic waves by Babich [4]. The main algorithms in ray tracing are defined as shooting and bending methods. The shooting approach utilizes a given initial direction and position for the ray and an interpolation tool to reach a certain point which is also known as initial-value method [5]. For modeling and imaging of complex structures by using shooting method, one can compute the multiple arrivals containing the most energetic wave which does not necessarily correlate to the first arrival. Sun and Schuster [6] employed the initial-value approach for the wave path migration. Julian [7] developed an



initial-value method to track rays in inhomogeneous media which is applied by Engdahl [8] for earthquake analysis.

An efficient alternative to compute traveltimes is solving the eikonal equation by employing finite differences [9, 10]. Although eikonal solvers only provide the first arrival times, they can compute traveltimes between two points. An attempt to extend eikonal solvers for obtaining multiple arrivals are conducted by Bevc [11]. Various techniques are introduced to acquire the solution of the eikonal equation comprising single-pass methods, embedding methods, sweeping methods and iterative methods [9]. The main difference of these techniques is that how they cope with the complication of multi-valued solutions, finding the solution in the vicinity of cusps and discontinuities [12]. Anisotropy is initially added to an eikonal solver algorithm by Dellinger and van Trier [13]. Fast sweeping methods are originally proposed for isotropic media [14], however, a modification is executed to handle the anisotropic condition [15]. Single-pass or fast marching method (FMM) is another tool to compute the traveltimes, though it is not generally applicable for anisotropic medium [10].

This paper presents the initial-value ray tracing and fast marching eikonal solver in isotropic and VTI media. An anelliptic VTI wave equation is used as a kernel of the ray tracing system. The ray tracing problem solved by a forth order Runge-Kutta integrator. The fast marching finite difference algorithm, which is used as our eikonal solver, belongs to the family of upwind finite difference schemes [16]. Although the ray tracing approach is able to compute multiple arrivals with great precision, the eikonal solver is faster and more stable for traveltime computation. We discuss the result of both approaches and compare them to choose the best applicable method for the further study.

## 2. Theory of initial-value ray tracing

The kernel of a ray tracing algorithm is the wave equation. Fomel [17] enhanced the anelliptic qP wave approximation proposed by Muir and Dellinger [18] through replacing the linear approximation with a nonlinear one. Using the shifted hyperbola approximation, he obtained the following approximation for P wave phase velocity:

$$v_p^2(\theta) \approx \frac{1}{2}e(\theta) + \frac{1}{2}\sqrt{e^2(\theta) + 4(q-1)ac\sin^2\theta\cos^2\theta} \quad (1)$$

where  $a = c_{11}$ ,  $c = c_{33}$ ,  $c_{ij}(X)$  are the density-normalized components of the elastic tensor,  $\theta$  is the phase angle between the phase direction  $n$  and the axis of symmetry, and  $q$  and  $e(\theta)$  are the anellipticity coefficient and the elliptical part of the velocity, respectively, defined by:

$$q = \frac{1+2\delta}{1+2\epsilon} = \frac{1}{1+2\eta} \quad (2)$$

and

$$e(\theta) = a\sin^2\theta + c\cos^2\theta. \quad (3)$$

Similarly, the shifted hyperbola approach is applied on the Muir's approximation to unlinearize the equation [17]. The new group velocity approximation is:

$$\frac{1}{v_p^2(\theta)} \approx \frac{1+2Q}{2(1+Q)}E(\theta) + \frac{1}{2(1+Q)}\sqrt{E^2(\theta) + 4(Q^2-1)AC\sin^2\theta\cos^2\theta} \quad (4)$$

where  $A = 1/a$ ,  $C = 1/c$ ,  $Q = 1/q$ ,  $\theta$  is the group angle, and  $E(\theta)$  is the elliptical part:

$$E(\theta) = A\sin^2\theta + C\cos^2\theta \quad (5)$$

The initial-value ray tracing is broadly utilized in the shooting method of two-point ray tracing [5]. In the one-point technique, an initial given point  $X_0$ , such as the source location, and an initial ray direction  $P_0$  are used to constitute the complete system of initial conditions for calculating the ray trajectory  $X(\sigma)$  and the traveltime along the ray  $T(\sigma)$ . By applying the initial values  $X(0) = X_0$ ,  $P(0) = P_0$ , and  $T(0) = 0$  in the ray tracing system

$$\frac{dX}{d\sigma} = P, \quad \frac{dP}{d\sigma} = S(X)\nabla S, \quad \frac{dT}{d\sigma} = S^2(X) \quad (6)$$

rays are obtained. Using the Euler's method, an approximate solution for the ray tracing problem can be achieved by taking a small step  $\Delta\sigma$  and advancing the solution according to:

$$X(\Delta\sigma) \approx X_1 = X_0 + P_0\Delta\sigma, \quad (7)$$

$$P(\Delta\sigma) \approx P_1 = P_0 + g(X_0)\Delta\sigma \quad (8)$$

where  $g(X) = S(X)\nabla S$  and  $S(X)$  is the slowness function. Continuing the first step leads to the iteration

$$X_k = X_{k-1} + P_{k-1}\Delta\sigma + g(X_{k-1})\frac{(\Delta\sigma)^2}{2} \quad (9)$$

$$P_k = P_{k-1} + \frac{g(X_{k-1}) + g(X_k)}{2}\Delta\sigma \quad (10)$$

and by using the third part of equation (6) and integrating a third order polynomial fitted at the end points of the  $\Delta\sigma$  interval together with its derivatives, traveltime  $T$  along the ray can be defined as:

$$T_N = \frac{S^2(X_0) + S^2(X_N)}{2}\Delta\sigma + \sum_{k=1}^{N-1} S^2(X_k)\Delta\sigma + \frac{g(X_0).P_0 - g(X_N).P_N}{6}(\Delta\sigma)^2. \quad (11)$$

The numerical solution of the ray tracing system can be carried out, with controlled accuracy, using different techniques such as the Runge-Kutta method and Hamming's predictor-corrector method. Iterative scheme 9 and 10 are a kind of the symplectic Runge-Kutta schemes, and we use a fourth order Runge-Kutta solver to determine rays.

### 3. Theory of fast marching eikonal solver

The fast marching method is using the fact that the direction of the energy propagation follows the group velocity equation, similar to a ray perpendicular to the wavefronts, which is defined by the phase velocity and it is called the traveltime gradient. We use equation 1 and 4 for ray tracing in locally homogeneous cells needed in this algorithm. An attentively selected order of traveltime evaluation is the main advantage of the fast marching method. While the algorithm is proceeding in a certain step, every grid point is labelled as either *Alive* (already computed), *NarrowBand* (at the wavefront, pending evaluation), or *FarAway* (not touched yet). In other words, at the beginning of the evaluation, the source positions are considered as *Alive*, and the time at these points is set to zero. A continuous band of points around the source are taken as *NarrowBand*, and their traveltime are computed analytically. Other points in the grid are marked as *FarAway* and have an "infinitely large" traveltime value [16]. The algorithm includes the following main steps:

1. Finding the point with the minimum traveltime among the *NarrowBand* points.
2. Label this point as alive.
3. Check all the immediate neighbors of the minimum point and update them if necessary
4. Repeat the procedure.

For updating, one to three neighbour points are selected which the traveltime values of them need to be smaller than the current value. After choosing the points, the below quadratic equation

$$\sum_j \left( \frac{t_i - t_j}{\Delta x_{ij}} \right)^2 = s_i^2 \quad (12)$$

should be solved for the updated value  $t_i$ .  $t_j$  are the traveltimes at the neighbouring points,  $s_i$  is the slowness at the point  $i$ , and  $\Delta x_{ij}$  is the grid size in the  $ij$  direction. The equation 12 is a finite difference approximation to the anisotropic eikonal equation [17]

$$v^2 \left( \frac{\nabla T}{|\nabla T|}, X \right) |\nabla T|^2 = 1 \quad (13)$$

where  $X$  is a point in space,  $T(X)$  is the travelt ime at that point for a given source, and  $v(n,X)$  is the phase velocity in the phase direction  $n = \frac{\nabla T}{|\nabla T|}$ .

#### 4. Numerical examples

We test the above-described algorithms for isotropic and VTI ray tracing and travelt ime computations in a 2D Marmousi model. The parameters that the Marmousi model (Figure 1) provides are vertical velocity  $V_{P0}$  and  $\eta = \frac{\varepsilon - \delta}{1 + 2\delta}$ . We use the slowness instead of the velocity to maximally preserve the travelt ime. The study is conducted on the seismic software package of Madagascar [19]. In the first example for the initial-value ray tracing, the source is located at  $x=0$  km and  $z=0$  km (Figure 2), and in the second example, the source is located at  $x=3$  km and  $z=0$  km (Figure 3).

We trace rays in the isotropic and anisotropic condition for the both cases. Since the ray tracing theory imposes some limitations on the subsurface model, to obtain valid rays both the true and an smoothed velocity model are studied. Smoothing is carried out by applying a tridiagonal  $2 \times 2$  filter for three times, and the ray window is  $100^\circ$  with a fan of 50 rays. It can be clearly seen that the rays traced via the anisotropic approach are well-ordered and smoother which causes a better coverage of the shadow zones than the isotropic one. Although, by smoothing the velocity, the result of the isotropic ray tracing is enhanced, the anisotropic rays of the smoothed model have a more reliable pattern and cover a wider area. We should mention that the anisotropic ray tracing is sensitive to smoothing and the smoothing parameters should not pass the threshold of the given velocity model.

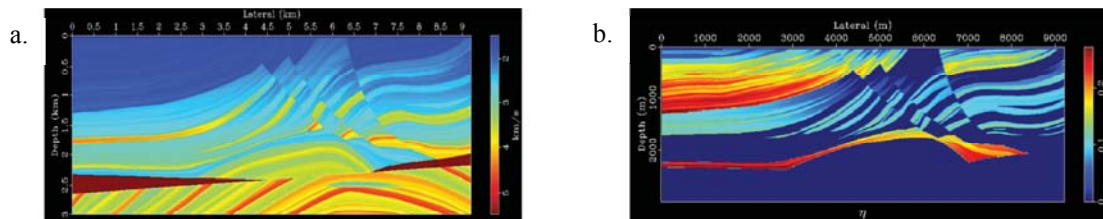


**Figure 1.** The Marmousi model: (a) vertical velocity model, (b) anelliptic  $\eta$  parameter.

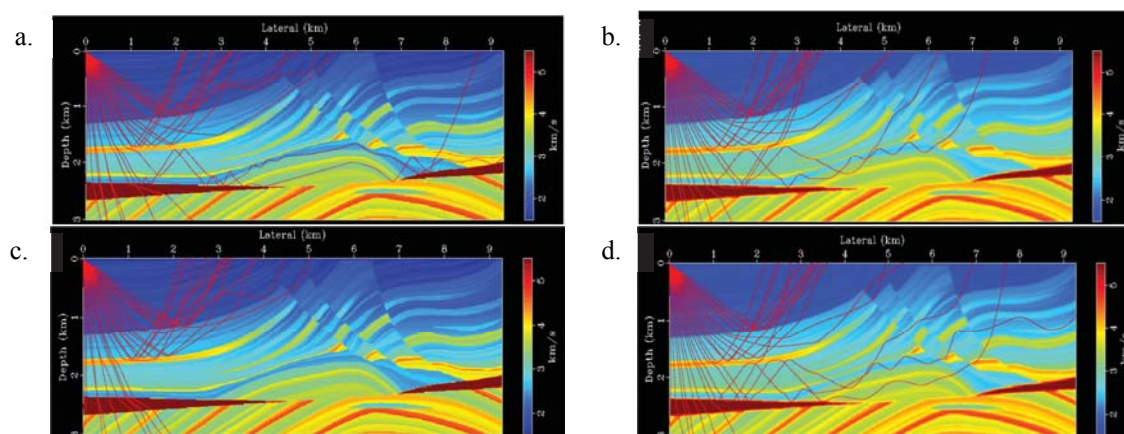


**Figure 2.** Initial-value ray tracing at  $x=0$  km: (a) isotropic in the true velocity, (b) isotropic in the smoothed velocity, (c) anisotropic in the true velocity and (d) anisotropic in the smoothed velocity.



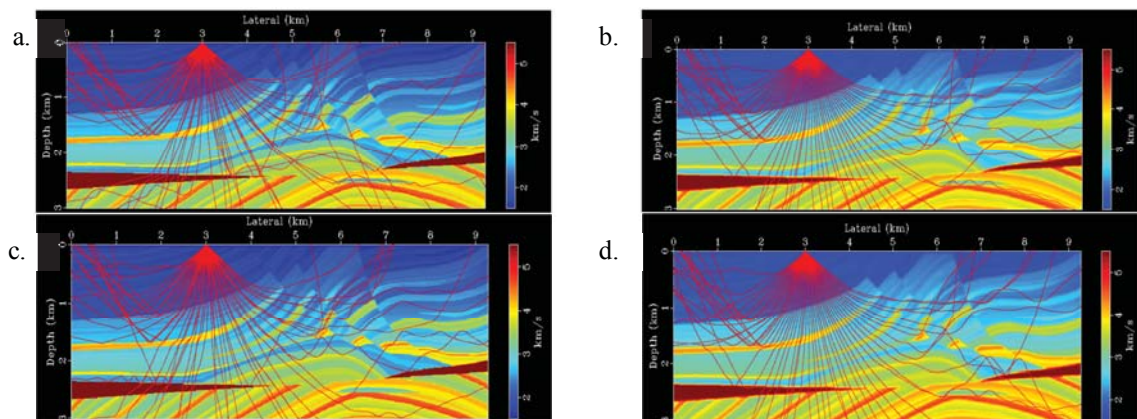


**Figure 3.** Initial-value ray tracing at  $x=3$  km: (a) isotropic in the true velocity, (b) isotropic in the smoothed velocity, (c) anisotropic in the true velocity and (d) anisotropic in the smoothed velocity.

The results of fast marching eikonal solver are illustrated in Figure 4. The first arrival traveltimes are computed in the anisotropic Marmousi model and compared with traveltimes contours of the isotropic Marmousi model. It can be clearly seen that anisotropic wavefronts laterally move faster than isotropic ones, however the isotropic and anisotropic wavefronts propagate in a same speed vertically. This difference demonstrates the significance of considering anisotropy in imaging. Ignoring the shift in wavefronts position can cause error in positioning.

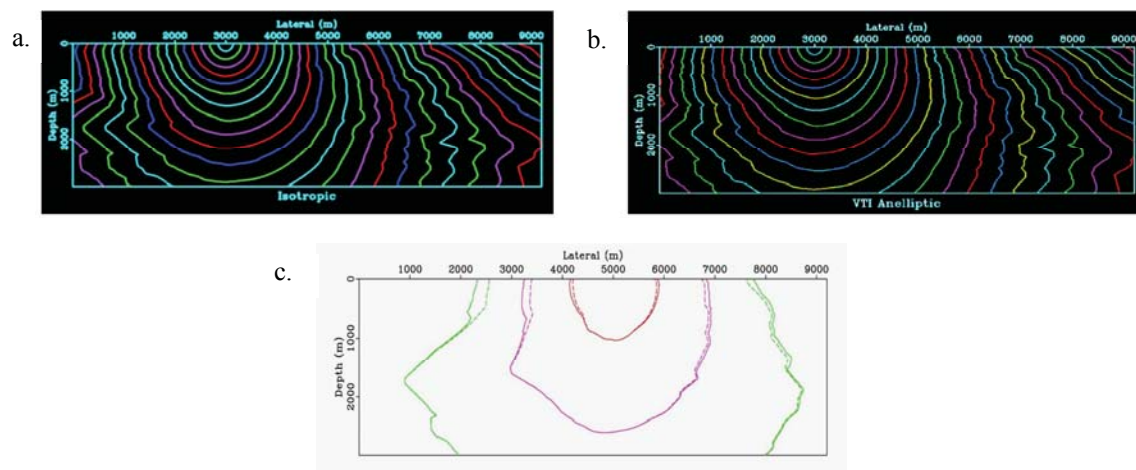


**Figure 4.** Fast marching traveltimes contours in: (a) isotropic Marmousi model, (b) anisotropic Marmousi model. (c) Comparison of isotropic and VTI traveltimes indicates a considerable difference between isotropic and anisotropic results.

Eventually, we present a comparison between VTI ray tracing and VTI fast marching methods (Figure 5). First, the exact solution and ray tracing result are overlaid to find out the accuracy of ray tracing approach. The overlaid figure shows overlapping the ray tracing approximation and exact solution which means a great accuracy for ray tracing algorithm. Then a same procedure is performed for fast marching result which indicates an small error for contours far from the source position, however, for near distances, the accuracy is high. Finally, we overlay the contour of both approaches. We can conclude that although applying the ray tracing technique is challenging in complex velocity models and is time consuming, it remains more accurate than finite difference technique in near and far offset.

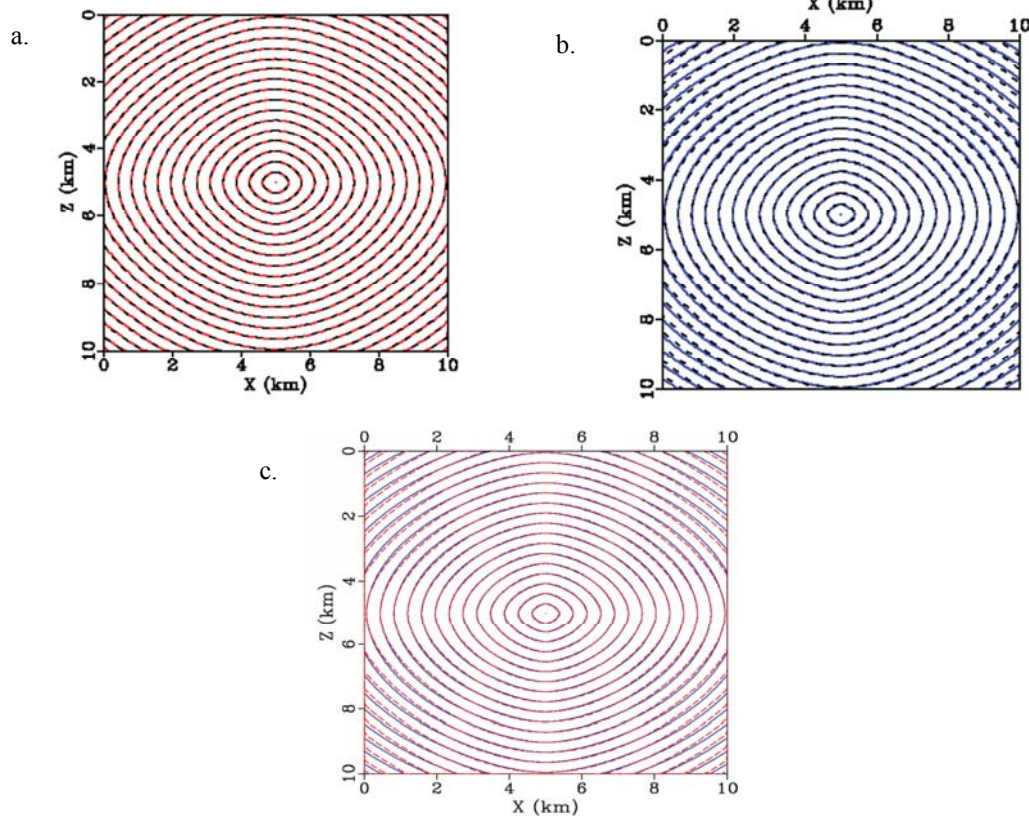


**Figure 5.** Comparison of VTI traveltimes between: (a) initial-value ray tracing (solid red) and exact solution (dashed black), (b) fast marching method (solid blue) and exact solution (dashed black), and (c) initial-value ray tracing (dashed red) and fast marching method (solid blue).

## 5. Conclusions

We studied two techniques of initial-value ray tracing and fast marching eikonal solver in isotropic and vertical transverse isotropy (VTI) media, and we compared the results for more evaluation. The rays traced via the anisotropic approach are well-ordered and smoother which causes a better coverage of the shadow zones than the isotropic one. Fast marching method proved that anisotropic wavefronts laterally move faster than isotropic ones, however the isotropic and anisotropic wavefronts propagate in a same speed vertically. This difference demonstrates the significance of considering anisotropy in imaging. Despite the high accuracy of the ray tracing algorithm to compute the traveltimes and providing the multiple arrivals, applying it in complex media is a challenging task and makes it excessively expensive for large-scale applications. On the other hand, the finite difference approach is fast and robust to define the traveltimes even in rough velocity media, though they only acquire first arrivals. Overall, since the ray tracing results are biased by the initial conditions and they are not deterministic explanations to problems, we cannot consider it as a long term solutions.

## Acknowledgements

This work is funded by the grant PETRONAS Petroleum Research Fund. The authors acknowledge the contribution of PETRONAS and Universiti Teknologi PETRONAS (UTP) staffs.

## References

- [1] L. Behera, *et al.*, 2011 "Anisotropic P-wave velocity analysis and seismic imaging in onshore Kutch sedimentary basin of India," *Journal of Applied Geophysics*, vol. 74, pp. 215-228
- [2] Z. Koren, *et al.*, 2008 "Anisotropic local tomography," *Geophysics*, vol. 73, pp. VE75-VE92

- [3] U. b. Waheed and T. Alkhalifah, 2013, "Efficient traveltimes solutions of the TI acoustic eikonal equation," in *75th EAGE Conference & Exhibition incorporating SPE EUROPEC 2013*.
- [4] V. Babich, 1956 "A RADIAL METHOD FOR COMPUTING THE INTENSITY OF WAVE FRONTS," *Doklady Akademii Nauk SSSR*, vol. 110, pp. 355-357
- [5] V. Cerveny, 2005 *Seismic ray theory*: Cambridge University Press.
- [6] H. Sun and G. T. Schuster, 2003 "3D wavepath migration," *Geophysical prospecting*, vol. 51, pp. 421-430
- [7] B. R. Julian, 1970 "Ray tracing in arbitrarily heterogeneous media," DTIC Document
- [8] E. R. Engdahl, 1973 "Relocation of intermediate depth earthquakes in the central Aleutians by seismic ray tracing," *Nature*, vol. 245, pp. 23-25
- [9] U. B. Waheed, *et al.*, 2015 "An iterative, fast-sweeping-based eikonal solver for 3D tilted anisotropic media," *Geophysics*, vol. 80, pp. C49-C58
- [10] J. A. Sethian and A. M. Popovici, 1999 "3-D traveltimes computation using the fast marching method," *Geophysics*, vol. 64, pp. 516-523
- [11] D. Bevc, 1997 "Imaging complex structures with semirecursive Kirchhoff migration," *Geophysics*, vol. 62, pp. 577-588
- [12] P. Sava and S. Fomel, 1998, "Huygens wavefront tracing: A robust alternative to ray tracing," in *SEG Technical Program Expanded Abstracts*, pp. 1961-1964.
- [13] J. Dellinger, 1991, "Anisotropic finite-difference traveltimes," in *Expanded Abstracts, Society of Exploration Geophysicists*, pp. 1530-1533.
- [14] H. Zhao, 2004 "A fast sweeping method for eikonal equation Mathematics of computation," *Providence, RI: American Mathematics of Society*
- [15] Y.-T. Zhang, *et al.*, 2006 "High order fast sweeping methods for static Hamilton–Jacobi equations," *Journal of Scientific Computing*, vol. 29, pp. 25-56
- [16] S. Fomel, 1997 "A variational formulation of the fast marching eikonal solver," *SEP-95: Stanford Exploration Project*, pp. 127-147
- [17] S. Fomel, 2004 "On anelliptic approximations for qP velocities in VTI media," *Geophysical Prospecting*, vol. 52, pp. 247-259
- [18] F. Muir and J. Dellinger, 1985 "A practical anisotropic system," *SEP-44*, vol. 55, p. 58.
- [19] S. Fomel, *et al.*, 2013 "Madagascar: open-source software project for multidimensional data analysis and reproducible computational experiments," *Journal of Open Research Software*, vol. 1, p. e8.